Journal of Photochemistry and Photobiology A: Chemistry 205 (2009) 104–108

Contents lists available at ScienceDirect

Journal of Photochemistry and Photobiology A: Chemistry

journal homepage: www.elsevier.com/locate/jphotochem

Cis–trans isomerization mechanism of 4-aminoazobenzene in the S_0 and S_1 states: A CASSCF and DFT study

Luoxin Wang*, Jie Xu, Hantao Zhou, Changhai Yi, Weilin Xu

Key Laboratory of Green Processing and Functional Textiles of New Textile Materials, Wuhan University of Science and Engineering, Ministry of Education, 1 FangZhi Road, Wuhan 430073, PR China

ARTICLE INFO

Article history:
Received 8 August 2008
Received in revised form 23 March 2009
Accepted 22 April 2009
Available online 3 May 2009

Keywords:
Aminoazobenzene
Isomerization mechanism
Potential energy surface
Ab initio

ABSTRACT

The isomerization mechanism of the ground-state and the first single excited-state (S_0 and S_1) for 4-aminoazobenzene (4-AAB) was studied on the basis of the DFT-B3LYP and CASSCF calculations. The results indicate that the thermal *cis–trans* ($E \leftrightarrow Z$) isomerization of 4-AAB mainly concerns the inversion mechanism, while the photoisomerization on the S_1 state involves the rotational pathway that is characterized by the S_1/S_0 conical intersection with a twisting structure. By means of the investigation on the geometrical parameters, it was found that the relaxation modes, which determine the decay dynamics of the excited states, are different for the *E*- and *Z*-isomers upon excited in the S_1 state. Moreover, the S_1 potential energy surface of 4-AAB is found to be similar to that of parent azobenzene. During the decay process of excited *E*-isomer through the rotation of the NN bond, however, the activation energy barrier of 4-AAB is lower than that of azobenzene, which suggests that the corresponding decay lifetime of S_1 excited *E*-4-AAB is smaller than that of *E*-azobenzene.

1. Introduction

Azobenzene (AB) and its derivatives have a typical characteristic of reversible *trans–cis* ($E \leftrightarrow Z$) isomerization, which has recently attracted significant interest in optical materials [1,2], media storage materials [3], light-triggered nano-machines [4,5], etc. Generally, two relative stable configurations (*E* and *Z*) can be observed in the electronic ground state of AB. Upon UV light (~365 nm) irradiation, *E*-AB can be converted to *Z*-AB. The $Z \rightarrow E$ backward isomerization can readily occur at room temperature and can be promoted by visible light irradiation.

Since two photoisomerization routes of AB being excited to different electronic states (see Fig. 1) were firstly proposed by Rau and Lüddecke [6], the photoisomerization mechanism of AB has been argued by many theoretical and experimental researchers [7–12]. Recently, some comprehensive studies tend to conclude that the rotation mechanism, which involves the rotation around the NN double bond, plays an important role in the $E \leftrightarrow Z$ isomerization process of AB on the $S_1(n \rightarrow \pi^*)$ and S_2 $(\pi \rightarrow \pi^*)$ states [13–17].

In contrast to the extensive study of AB, there are few reports concerning the photoisomerization of substituted AB. In fact, the presence of substituents may modify the electronic structure and excited energy of azobenzene [18]. It is possible that the photoisomerization mechanism and dynamics of the substituted azobenzene are different from those of parent azobenzene. Sub-picosecond time-resolved absorption spectroscopy has shown that there exists a remarkable substituent effect on the decay dynamics of excited states for the donor–acceptor 4,4′-substituted *E*-azobenzene [19]. In our previous work [20], the potential energy surfaces of the S_0 and S_1 were mapped for 4-amino-4′-nitroazobenzene (ANAB) and 4-amino-4′-cyanoazobenzene (ACAB) on the basis of the CASSCF calculations. The result indicates that the photoisomerization on the S_1 state mainly involves the rotation mechanism for both ANAB and ACAB. Upon being excited to the S_2 state or vibrationally hot S_1 state, however, the inversion channel could be accessible to decay the excited electron's energy. The calculation result also indicates that different electron-withdrawing groups (e.g. $-NO_2$, –CN) on 4-position can modify the conical intersection lying on the inversion decay pathway. UV–vis transient absorption spectroscopy carried out on 4-aminoazobenzene (4-AAB) has shown that the potential energy gap between the S_1 $(n \rightarrow \pi^*)$ and S_2 $(\pi \rightarrow \pi^*)$ states plays a key role to determine the *E–Z* photoisomerization dynamics of azobenzene derivatives [21].

In this work, we chose the 4-aminoazobenzene(4-AAB) as the model molecule and performed the DFT and CASSCF calculations to optimize the structures and scan the potential energy surfaces (PES) of S_0 and S_1 states. Our aim is to shed light on the effect of electronic donor substituent on the photoisomerization mechanism and decay dynamics of azobenzene.

* Corresponding author. Tel.: +86 27 87426559; fax: +86 27 87426559.
E-mail address: wanglx@wuse.edu.cn (L. Wang).

1010-6030/$ – see front matter © 2009 Elsevier B.V. All rights reserved.
doi:10.1016/j.jphotochem.2009.04.014

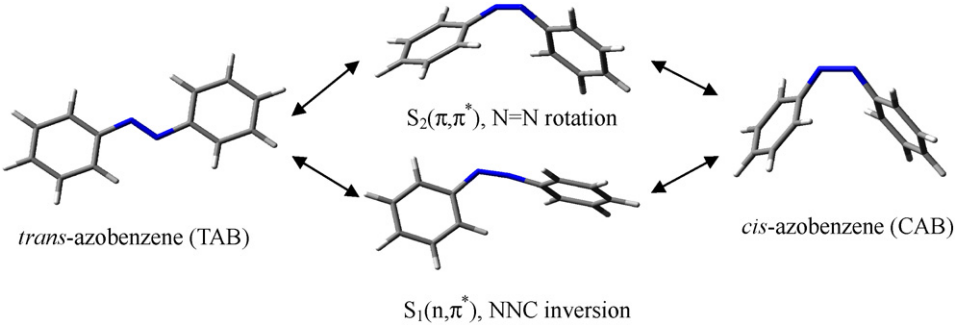

Fig. 1. Traditional inversion versus rotation mechanisms of azobenzene photoisomerization.

2. Calculation details

The stable *E*- and *Z*-isomers and the transition states for the thermal isomerization of 4-AAB in S_0 state were optimized unrestrainedly by means of the DFT and CASSCF methods. These optimized structures were confirmed to be the minimum-energy points or first-order saddle points by vibrational frequency calculations. The optimization of the critical points on S_1 state and the relaxed S_1 PES scan along the CNNC dihedral were performed by the state-specific CASSCF calculation. The state-average CASSCF method was used to determine the geometry in the intersection space of S_0 and S_1 states. The 6-31G* basis set was used in the B3LYP and CASSCF calculations. All the calculations were performed by using Gaussian 03 program package [22].

In principle, all of the valence electrons and orbitals should be included in the active space for the CASSCF calculations. Practically, until now it is not possible for the azobenzene because of the limitation of software and computational capability. So the selection of the active space is a crucial step in a CASSCF calculation. According to the previous calculations of azomethane [23] and the donor–acceptor 4,4′-substituted azobenzene [20], the active space should at least include six electrons distributed among four orbitals, referred as to CAS(6,4), which can reasonably describe the S_1 PES of photoisomerization. In our study on the 4-AAB, we chose an active space of twelve electrons in ten orbitals, namely CAS(12,10), in order to reasonably map the PES of photoisomerization on the excited state. These orbitals correspond to the nitrogen's π and π^* orbitals, their two non-bonding orbitals occupied by two lone-pair electrons ($n+$, $n-$) and three π and π^* orbitals of the benzenic orbital.

3. Results and discussion

It has been found that adding the substituents, especially the electron-donor or acceptor groups, can lead to lower the S_2 ($\pi \rightarrow \pi^*$) excitation energy of azobenzene but has little influence on the S_1 ($n \rightarrow \pi^*$) excitation energy [18]. With respect to azobenzene, 4-AAB has a small potential energy gap between the S_1 and S_2 states due to the existence of amino group in the molecular structure. Once excited to the S_2 state, 4-AAB can rapidly degenerate from the S_2 state to the S_1 state by way of the internal conversion and the isomerization process occurs mainly on the S_1 and S_0 states. In the present research, therefore, we focused on the isomerization mechanisms on the S_0 and S_1 states.

Being different from azobenzene (C_{2h} symmetry), 4-AAB is an asymmetrical molecule due to the presence of amino group. For brevity, the phenyl ring substituted by $-NH_2$ group is labeled as α-Ph and the other one without substituent is labeled as β-Ph, as is shown in Fig. 2. The asymmetric CN bonds, CNN angles and NNCC dihedrals locating on both sides of azo group are also marked as "α-" and "β-" correspondingly.

3.1. Molecular geometries

The geometrical parameters of 4-AAB, optimized by the B3LYP/6-31G* and CAS(12,10)/6-31G* level of theory, respectively, are presented in Table 1. The molecular backbone of *E*-4-AAB calculated at the B3LYP/6-31G* level is a planar structure, whereas the two hydrogen atoms of the $-NH_2$ group are out of the molecular plane because of the existence of the lone-pair electrons on the nitrogen of $-NH_2$. The optimized *Z*-isomer is nonplanar and the two phenyl rings twist around the NC bonds to some degree. The theoretical calculations of azobenzene have indicated that the structural parameters optimized at the B3LYP/6-31G* level are comparable to the experimental data [24–26], thus it is reasonable to compute the structure of 4-AAB with the same theoretical method and basis set.

As shown in Table 1, it can be found that some geometries of *E*-AAB and *Z*-AAB optimized by the CAS(12,10)/6-31G* method are very close to the results by the B3LYP/6-31G* method. For example, the two calculation methods give the very similar values of the CNN bond angles and NNCC dihedrals. The differences in the CN bond lengths are lower than 0.015 Å. Only the CASSCF NN bond length is shorter of 0.023 Å than the DFT value. The means that the CAS(12,10)/6-31G* method can also give the relatively reasonable structure parameters of 4-AAB.

For the $E \leftrightarrow Z$ isomerization in the ground state of 4-AAB, three transition states, referred as to $TS_{0/rot}$, α-$TS_{0/inv}$ and β-$TS_{0/inv}$, were obtained on the basis of B3LYP and CASSCF calculations. Vibrational frequency calculations give only one imaginary frequency for these transition states. These frequencies correspond to the twisting of CNNC dihedral and the bending of α-CNN angle and β-CNN angle, respectively. Similar to the case of azoalkane and diazetines [27], the B3LYP calculation was also found to fail in optimizing structure of $TS_{0/rot}$ of 4-AAB.

In comparison with the structures of *E*-4-AAB, the NN bond length of $TS_{0/rot}$, which is optimized at the CAS(12,10)/6-31G* level of theory, is elongated about ~0.096 Å and the β-CN bond length decreases significantly (0.08 Å). The change in the α-CN bond is relatively small (only about 0.03 Å). This can be explained by the fact that the conjugated π-bond of azo group is broken due to the twist-

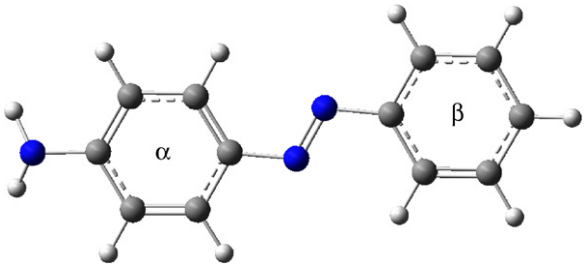

Fig. 2. Molecular structure of 4-AAB.

Table 1
Optimized geometrical parameters of 4-AAB on the S_0 and S_1 potential energy surfaces with different computational methods.

	Bond length (Å)			Angle (degree)				
	NN	CN (α-, β-)		CNN (α-, β-)		CNNC	NNCC (α-, β-)	
B3LYP/6-31G* calculation								
E-AAB (S_0)	1.265	1.407	1.418	115.3	114.6	179.9	0.1	0.1
Z-AAB (S_0)	1.253	1.427	1.433	125.0	124.4	10.4	36.2	56.4
α-$TS_{0/inv}$	1.242	1.334	1.450	178.8	116.7	121.0	104.5	4.3
β-$TS_{0/inv}$	1.230	1.435	1.332	117.6	179.5	−176.9	0.20	87.3
CAS(12,10)/6-31G* calculation								
E-AAB (S_0)	1.242	1.422	1.423	115.4	115.0	180.0	0.13	0.03
Z-AAB (S_0)	1.242	1.434	1.435	123.5	123.2	4.6	54.8	62.8
$TS_{0/rot}$	1.338	1.396	1.346	116.8	119.0	88.9	3.4	0.18
$S_{1/min}$	1.258	1.391	1.358	126.8	129.5	179.6	0.04	0.1
TS_1	1.259	1.385	1.387	131.3	123.0	116.4	10.9	2.2
CI_{rot}	1.272	1.414	1.358	117.4	134.5	92.0	9.5	1.7
Rotamer-S_1_170.0	1.258	1.391	1.359	126.8	129.3	170.0	3.67	1.39
Rotamer-S_1_110.0	1.270	1.377	1.387	136.0	120.6	110.0	15.4	0.5
Rotamer-S_1_70	1.267	1.377	1.386	138.0	120.1	70.0	14.9	2.9
Rotamer-S_1_10	1.240	1.393	1.350	144.5	132.9	10.0	60.4	0.34

ing of the NN double bond and that the π-electrons delocalizing into the phenyl rings result in the decrease in the electron-cloud density of the NN bond and the increase in the electron-cloud density of the two CN bonds.

The α-$TS_{0/inv}$ is formed by the α-CNN angle inversion to about 180°. As the α-CNN angle inverts, the orbital of α-N atom occurs the $sp^2 \rightarrow sp$ rehybridization, which causes the evident compression of α-CN bond length. Inversion of the α-CNN angle does not induce the significant change of the β-CNN bond angle, only results in a slight compression of the NN bond and the elongation of the CN bond. The similar trend can be observed in the β-$TS_{0/inv}$ formed by the inversion of β-CNN angle.

For both α-$TS_{0/inv}$ and β-$TS_{0/inv}$, it is worth noted that the two phenyl rings of the transition states are not coplanar, but close to perpendicular to each other. This result indicates that the thermal-inversion isomerization process involves the rotation of the phenyl rings.

According to the changes in the geometries of 4-AAB upon excitation to the S_1 state, the relaxation process from the Frank–Condon (FC) point to the S_1/S_0 conical intersection (CI) can be separated into three stages. The structural parameters of $S_{1/min}$, TS_1 and some important rotamer-S_1 are shown in Table 1. For the excited *E*-isomer, the initial relaxation mainly involves the NN bond stretching, the two CN bonds compressing and the CNN angle opening. The following decay is characterized by the twist of the CNNC dihedral angle. During the CNNC rotation from 170° to 110°, the NN and β-CN bond length and α-CNN angle become larger. The β-CN bond length becomes smaller. Finally, the decay in the S_1/S_0 intersection space is related to the stretching of the NN and α-CN bonds as well as the bending of the CNN angles.

For the excited *Z*-isomer, the relaxation mode is different from the case of the *E*-isomer. The initial changes of geometries concern the significant decrease in the CN bond lengths and the increase in CNN angles. Along with the CNNC dihedral twisting from 10° to 70°, the NN bond and β-CN bond lengths further increase and the two CNN angles and α-CN bond length decrease, while the α-phenyl ring rotates evidently. The final relaxation in the intersection space involves the stretch of the corresponding bonds and the further compression of the bond angles. The different relaxation modes of the *E*- and *Z*-isomers give rise to the different decay lifetimes and energy changes, which is verified by the following relaxed-PES scan.

From the CI_{rot} to the $TS_{0/rot}$, this decay process concerns the vibrational coupling of the corresponding bonds. The molecular structure of CI_{rot} is characterized by the CNNC dihedral angle of 92.0°. This twist geometry means that the rotation mechanism mainly operates on the S_1 state for the photoisomerization of 4-AAB.

3.2. Analysis of the PES

The potential energy surfaces of the S_0 and S_1 states along the CNNC rotational coordinate are shown in Fig. 3. The relative energies of several key points are summarized in Table 2. The B3LYP/6-31G* and CAS(12,10)/6-31G* calculations give the very similar energy difference (~16 kcal/mol) between the *Z*- and *E*-isomers of 4-AAB. The energy difference of 4-AAB is also very close to that of the azobenzene (~15 kcal/mol) [15,25], which indicates that the substituent of amino does not evidently influence the relative thermal stability of the *Z*- and *E*-isomers.

The relative energy order of the three transition states is as following: α-$TS_{0/inv}$ > $TS_{0/rot}$ > β-$TS_{0/inv}$. Evidently, the thermal isomerization through the inversion of β-CNN angle is the most favorable pathway in energy. The thermal isomerization mechanism of azobenzene and its derivatives has been investigated extensively from the experimental and theoretical viewpoints [10,28–31]. All the calculation results suggest that the inversion mechanism plays a key role in the thermal isomerization of azobenzene and its derivatives. Our calculation result also supports this inversion mechanism.

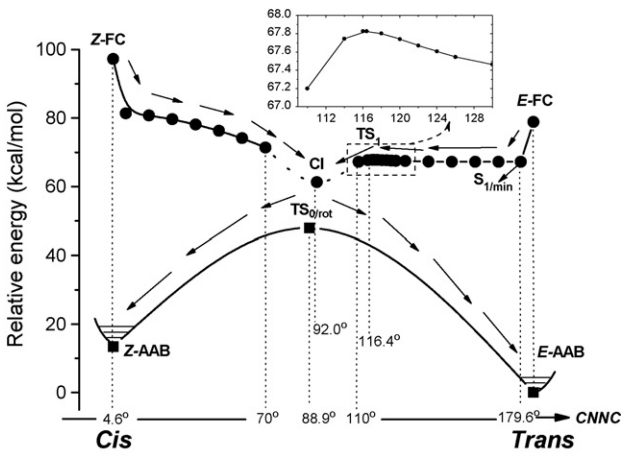

Fig. 3. Potential-energy surfaces of S_0 and S_1 states for 4-AAB along the CNNC torsional coordinates. The dashed frame is magnified in the inset in order to show the potential energy evolution in the vicinity of TS_1.

Table 2
Total energies and relative energies of some key points on the S_0 and S_1 potential energy surfaces of 4-AAB.

	Total energy (a.u.)	Relative energy (kcal/mol)	ZPE (kcal/mol)	Imaginary frequency (cm^{-1})
(TD-)B3lYP/6-31G* calculation				
E-AAB (S_0)	−628.11824	0.0	130.4	–
Z-AAB (S_0)	−628.09282	15.7	130.2	–
α-$TS_{0/inv}$	−628.04757	42.8	128.9	463.1
β-$TS_{0/inv}$	−628.05470	38.4	128.9	417.3
E-FC (S_1)	–	60.7[a]	–	–
Z-FC (S_1)	–	74.5[a]	–	–
CAS(12,10)/6-31G* calculation				
E-AAB (S_0)	−624.22283	0	139.7	–
Z-AAB (S_0)	−624.20139	13.5	139.6	–
E-FC (S_1)	−624.09712	78.9[a]	–	–
Z-FC (S_1)	−624.06791	97.2[a]	–	–
$TS_{0/rot}$	−624.14220	47.9	137.0	943.8
α-$TS_{0/inv}$	−624.14025	49.0	136.9	564.6
β-$TS_{0/inv}$	−624.14776	43.6	136.2	328.9
$S_{1/min}$	−624.11582	66.9	139.5	–
TS_1	−624.11470	67.0	138.8	156.4
CI_{rot}	−624.125211 (S_0) −624.125182 (S_1)	61.3[a]	–	–

[a] Without ZPE correction.

Additionally, it should be noted that the energy differences between the $TS_{0/rot}$ and β-$TS_{0/inv}$ is not very large (only ∼4 kcal/mol), thus it cannot be excluded that the thermal isomerization occurs possibly by means of the twist of the CNNC dihedral. On the other hand, in view of the structure of β-$TS_{0/inv}$, one of the phenyl rings rotates significantly. Therefore, it is expected that the CNNC dihedral will twist in the initial stage of the thermal isomerization process.

In fact, the early experiments about the 4-(diethylamino) azobenzene have shown that the thermal isomerization mechanism and rate are associated with the reaction conditions (solvent, temperature, pressure, etc.) and that the inversion and rotation mechanisms may compete with each other during the thermal isomerization process [32–34]. Our calculation result is not in conflict with these experimental observations.

As shown in Table 2, the first vertical excitation energy of *E*-4-AAB computed by the TD-DFT method is 60.7 kcal/mol (∼2.63 eV), in good agreement with the result (2.59 eV) of SOPPA calculation [18]. The CAS(12,10)/6-31G* excitation energy is 78.9 kcal/mol, which is about 18.2 kcal/mol greater than the DFT energy. Generally, the CASSCF calculation overestimates the transition energy because dynamic correlation energy is not included. This trend also occurs in the case of azobenzene [13,35].

As for the S_1 PES shown in Fig. 3, a distinct difference appears between the potential energy evolutions of the excited *E*- and *Z*-isomers. The surface from the *E*-FC down to the CI is rather flat except for the initially rapid energy decay. For the *Z*-isomer, however, it can be found that the potential energy decreases relatively fast. This discrepancy probably determines the decay dynamics of the excited *E*- and *Z*-isomers. The relevant experimental study still needs to be considered in detail.

The profile of the above S_1 PES of 4-AAB is very similar to that of azobenzene reported by Cembran et al. [13]. A local minimum ($S_{1/min}$) and a transition state (TS_1) have been found on the S_1 state. The local minimum is approximately a planar geometry with the CNNC dihedrals of 179.6°. Its N=N bond is slightly stretched and the two C–N bonds are shortened significantly with respect to the corresponding *E*-FC point. The N=N bond increases from 1.242 to 1.258 Å and the two C–N bond distances change about 0.03–0.07 Å. Furthermore, a large increase of over 12° in the CNN angles is observed. The $n \rightarrow \pi^*$ excitation results in a fractional rehybridization of azo nitrogen atoms from sp^2 to sp. As a consequence, the π-bonding character of C–N bond is enhanced and the two CNN angles open up significantly. The above bond parameter changes are presumably responsible for the energy decay from the FC point to the local minimum in the S_1 state.

The transition state structure on the S_1 state of 4-AAB is characterized by the CNNC angle of about 116.4°, while the other geometrical parameters related to the azo group are close to those of the $S_{1/min}$. Force-constant calculations indicated that this transition state involves only one imaginary frequency corresponding to the twist of CNNC dihedral. The CASSCF energy of TS_1 is higher of only ∼0.7 kcal/mol than that of $S_{1/min}$. This energy barrier further decreases to ∼0.1 kcal/mol when the zero-point energy (ZPE) correction is included. The activation energy barrier on the S_1 surface of 4-AAB is found to be lower than the barrier on the S_1 surface of AB (∼2 kcal/mol) [13].

The transition state existing on the S_1 PES should not alter the rotation mechanism of photoisomerization for 4-AAB and AB because the activation energy barrier is very small. However, the magnitude of activation energy barrier probably has influence on the decay dynamics of excited 4-AAB and AB. The small barrier means that the excited *E*-4-AAB can decay to CI more rapidly than the excited *E*-AB through the rotation of the NN bond. As a matter of fact, the observed transient absorption of the S_1 state decays double-exponentially with lifetimes of 0.6 and 1.9 ps for the *E*-4-AAB [21], while the *E*-AB decays in a biphasic fashion with time constants of 0.34 and 3.0 ps [36]. Lednev et al. [37] also found that *E*-AB decays with lifetimes of 0.6 and 2.5 ps. According to the explanation by Cembran et al. [13], the subpicosecond decay of transient absorption is associated with the vibrational energy redistribution starting from the FC point and the slower decay is related to the subsequent motion searching for the CI. There is a small energy barrier to be overcome during the relaxation process of excited *E*-4-AAB, thus the decay lifetimes of *E*-4-AAB are smaller than those of *E*-AB. Our calculation results give evidence in support of the difference in the decay dynamics of 4-AAb and AB.

When further scanning the S_1 PES along the CNNC dihedral that was changed from 70° to 110°, we encountered the wave-function convergence problem during the process of optimization with the state-specific CASSCF method. This convergence problem might be an indication of a coupling between the S_1 and S_0 states, which means that the conformers with the CNNC dihedral of 70–110° locate in the surface crossing region (the dashed line connecting the CI, shown in Fig. 3). The conical intersection, as an efficient photochemical funnel, determines the photoisomerization mechanism of 4-AAB. The optimized CI has a twisting structure and lies in the middle part of the S_1 PES along the CNNC rotation coordinate. These

results provide sufficiently evidence that the photoisomerization of 4-AAB on the S_1 excited state takes place by means of the rotation mechanism.

The S_2 ($\pi \rightarrow \pi^*$) state excitation, which corresponds to a maximum intensity for azobenzene and its derivatives, is often applied to induce the photoresponsive properties of the relevant materials. So, the photoisomerization dynamic and mechanism on the S_2 state should be more practical. The work considering the effect of different substituents (e.g. $-NH_2$, NO_2, etc.) on the photoisomerization of azobenzene on the S_2 state is under way.

4. Conclusion

In this work, the B3LYP/6-31G* and CAS(12,10)/6-31G* calculations show that the inversion mechanism is preferred and the CNN angle on the side of phenyl ring without $-NH_2$ readily opens up in the thermal-isomerization process of 4-AAB. However, the rotation mechanism cannot be excluded because the activation energy barrier of rotation pathway is only about 4 kcal/mol higher that that of inversion route. Similar to the azobenzene, the rotational pathway is the most possible photoisomerization channel for the S_1 state of 4-AAB. The excited *E*- and *Z*-4-AAB show different relaxation modes, which concern the different evolutions of geometrical parameters and energy. It is also found that the activation energy barrier for *E*-4-AAB decaying from FC point to CI is lower than the barrier for *E*-AB, which suggests that the excited *E*-4-AAB can decay more rapidly than the excited *E*-AB through the rotation of the NN bond.

Acknowledgment

The research was supported by the Key Project of Chinese Ministry of Education (Grant No. 209080).

References

[1] X.G. Wang, J. Kumar, S.K. Tripathy, L. Li, J.I. Chen, S. Marturunkakul, Macromolecules 30 (1997) 219–225.
[2] X.G. Wang, J.I. Chen, S. Marturunkakul, L. Li, J. Kumar, S.K. Tripathy, Chem. Mater. 9 (1997) 45–50.
[3] T. Ikeda, O. Tsutsumi, Science 268 (1995) 1873–1875.
[4] Y.L. Yu, M. Nakano, T. Ikeda, Nature 425 (2003) 145.
[5] T. Hugel, N.B. Holland, A. Cattani, L. Moroder, M. Seitz, H.E. Gaub, Science 296 (2002) 1103–1106.
[6] H. Rau, E. Lüaddeke, J. Am. Chem. Soc. 104 (1982) 1616–1620.
[7] Y. Norikane, N. Tamaoki, Eur. J. Org. Chem. 5 (2006) 1296–1302.
[8] H. Satzger, C. Root, M. Braun, J. Phys. Chem. A 108 (2004) 6265–6271.
[9] T. Schultz, J. Quenneville, B. Levine, A. Toniolo, T.J. Martinez, S. Lochbrunner, M. Schmitt, J.P. Shaffer, M.Z. Zgierski, A. Stolow, J. Am. Chem. Soc. 125 (2003) 8098–8099.
[10] C.R. Crecca, A.E. Roitberg, J. Phys. Chem. A 110 (2006) 8188–8203.
[11] T. Ikegami, N. Kurita, H. Sekino, Y. Ishikawa, J. Phys. Chem. A 107 (2003) 4555–4562.
[12] C. Ciminelli, G. Granucci, M. Persico, Chem. Eur. J. 10 (2004) 2327–2341.
[13] A. Cembran, F. Bernadi, M. Garavelli, L. Gagliardi, G. Orlandi, J. Am. Chem. Soc. 126 (2004) 3234–3243.
[14] E.W.G. Diau, J. Phys. Chem. A 108 (2004) 950–956.
[15] L. Gagliardi, G. Orlandi, F. Bernardi, A. Cembran, M. Garavelli, Theor. Chem. Acc. 111 (2003) 363–372.
[16] C.W. Chang, Y.C. Lu, T.T. Wang, E.W.G. Diau, J. Am. Chem. Soc. 126 (2004) 10109.
[17] I. Conti, M. Garavelli, G. Orlandi, J. Am. Chem. Soc. 130 (2008) 5216–5230.
[18] P.S. Ramanujam, P.-O. Astrand, S. Hvilsted, K.L. Bak, S.P.A. Sauer, J. Am. Chem. Soc. 122 (2000) 3482–3487.
[19] M. Hagiri, N. Ichinose, C. Zhao, H. Horiuchi, H. Hiratsuka, T. Nakayama, Chem. Phys. Lett. 391 (2004) 297–301.
[20] L.X. Wang, X.G. Wang, J. Mol. Struct. (THEOCHEM) 847 (2007) 1–9.
[21] Y. Hirose, H. Yui, T. Sawada, J. Phys. Chem. A 106 (2002) 3067–3071.
[22] M.J. Frisch, G.W. Trucks, H.B. Schlegel, G.E. Scuseria, M.A. Robb, J.R. Cheeseman, J.A. Montgomery, Jr., T. Vreven, K.N. Kudin, J.C. Burant, J.M. Millam, S.S. Iyengar, J. Tomasi, V. Barone, B. Mennucci, M. Cossi, G. Scalmani, N. Rega, G.A. Petersson, H. Nakatsuji, M. Hada, M. Ehara, K. Toyota, R. Fukuda, J. Hasegawa, M. Ishida, T. Nakajima, Y. Honda, O. Kitao, H. Nakai, M. Klene, X. Li, J.E. Knox, H.P. Hratchian, J.B. Cross, C. Adamo, J. Jaramillo, R. Gomperts, R.E. Stratmann, O. Yazyev, A.J. Austin, R. Cammi, C. Pomelli, J.W. Ochterski, P.Y. Ayala, K. Morokuma, G.A. Voth, P. Salvador, J.J. Dannenberg, V.G. Zakrzewski, S. Dapprich, A.D. Daniels, M.C. Strain, O. Farkas, D.K. Malick, A.D. Rabuck, K. Raghavachari, J.B. Foresman, J.V. Ortiz, Q. Cui, A.G. Baboul, S. Clifford, J. Cioslowski, B.B. Stefanov, G. Liu, A. Liashenko, P. Piskorz, I. Komaromi, R.L. Martin, D.J. Fox, T. Keith, M.A. Al-Laham, C.Y. Peng, A. Nanayakkara, M. Challacombe, P.M.W. Gill, B. Johnson, W. Chen, M.W. Wong, C. Gonzalez, J.A. Pople, Gaussian 03 Revision E.01; Gaussian, Inc., Wallingford, CT, 2005.
[23] R. Liu, Q. Cui, K.M. Dunn, K. Morokuma, J. Chem. Phys. 105 (1996) 2333–2345.
[24] N. Biswas, S. Umapathy, J. Phys. Chem. A 101 (1997) 5555–5566.
[25] N. Kurita, S. Tanaka, S. Itoh, J. Phys. Chem. A 104 (2000) 8114–8120.
[26] T. Takemasa, T. Hiroyuki, T. Hiroshi, E. Toru, K. Shigehiro, J. Phys. Chem. A 105 (2001) 9347–9353.
[27] Y. Shinichi, M. Tsutomu, J. Phys. Chem. A 105 (2001) 7281–7286.
[28] L.X. Wang, X.G. Wang, J. Mol. Struct. (THEOCHEM) 806 (2007) 179–186.
[29] K. Baba, H. Ono, E. Itoh, S. Itoh, K. Noda, T. Usui, K. Ishihara, M. Inamo, H. Takagi, T. Asano, Chem. Eur. J. 12 (2006) 5328–5333.
[30] O. Kikuchi, M. Azuki, Y. Inadomi, K. Morihashi, J. Mol. Struct. (THEOCHEM) 468 (1999) 95–99.
[31] J. Henzl, M. Mehlhorn, H. Gawronski, K.H. Rieder, K. Morgenstern, Angew. Chem. Int. Ed. 45 (2006) 603–606.
[32] T. Asano, T. Okada, S. Shinkai, K. Shigematsu, Y. Kusano, O. Manabe, J. Am. Chem. Soc. 103 (1981) 5161–5165.
[33] T. Asano, J. Am. Chem. Soc. 102 (1980) 1205–1206.
[34] D.M. Shin, D.G. Whitten, J. Am. Chem. Soc. 110 (1988) 5206–5208.
[35] L.X. Wang, W.L. Xu, C.H. Yi, X.G. Wang, J. Mol. Graph. Model. 27 (2009) 792–796.
[36] H. Satzger, S. Spörlein, C. Root, J. Wachtveitl, W. Zinth, P. Gilch, Chem. Phys. Lett. 372 (2003) 216–223.
[37] I.K. Lednev, T.-Q. Ye, P. Matousek, M. Towrie, P. Foggi, F.V.R. Neuwahl, S. Umapathy, Chem. Phys. Lett. 290 (1998) 68–74.